Precision & Performance Conference 2025, Cranfield University, UK, 18th- 20th November 2025

Combined planar and non-planar path planning for wire arc additive manufacturing of an organic bow window in AlSi5: slicing optimization and process prototyping.

Atif Naseer , Francesca Paradiso, Barbara Previtali

Department of Mechanical Engineering, Politecnico di Milano, Via Privata Giuseppe La Masa, 1, 20156 Milano MI, Italy.

atif.naseer@polimi.it

Abstract

The convergence of digital design and large-scale additive manufacturing presents new challenges in ensuring manufacturability of geometrically complex components. This research introduces a custom-built, visually programmed slicing and path-planning workflow, specifically tailored for Wire Arc Additive Manufacturing (WAAM) of bespoke products. Focusing on a Bow Window prototype with overhang-prone features, particularly Y-shaped junctions, the workflow enables manual switching between planar and non-planar slicing strategies to improve deposition quality. While not dynamically adaptive, the method empowers the designer to embed process constraints into the early design-to-fabrication pipeline, aligning closely with design-for-manufacturing (DFM) principles. The resulting improvement in the printability and structural continuity of critical overhang regions demonstrates the potential of this approach for extending WAAM's applicability in complex, product-scale fabrication. Among the discussed approaches, the optimized one enabled for lower dimensional error and areal surface roughness relative to conventional approach.

Design for Manufacturing (DFM), Wire Arc Additive Manufacturing (WAAM), Non-Planar Slicing, Aluminium AlSi5, Bow Window

1. Introduction

Wire Arc Additive Manufacturing (WAAM) is a Directed Energy Deposition (DED) process distinguished by its high deposition rates [1], making it one of the most viable additive manufacturing methods for large-scale production. However, the absence of support structures in WAAM poses challenges for printing overhanging features, often leading to common defects such as excessive overhang deformation, inconsistent material deposition (macro-voids), and staircase effects caused by conventional slicing techniques [2].

This research presents a custom-developed slicing and path-planning workflow built using visual programming, specifically tailored for WAAM of bespoke geometries. The workflow is applied to a Bow Window concept design [2] that includes overhang-prone features, particularly Y-shaped junctions, and allows for manual switching between planar and non-planar slicing strategies to enhance deposition quality.

The concept design and corresponding representative geometry of Y-shaped junction slicing is shown in figure 1. The effectiveness of this adaptive approach is validated through iterative printing trials, which are subsequently analysed to derive insights into design guidelines and path-planning strategies for WAAM. The following sections detail the methodology, followed by results from prototyping with AlSi5, and the key lessons learned from iterative fabrication.

2. Methodology

This study adopts a geometry-driven methodology for slicing and path planning tailored for large-scale WAAM fabrication.

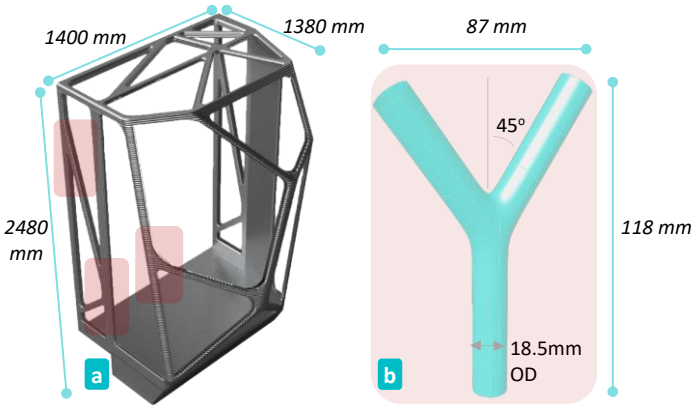

Figure 1. a) Bow window Concept Design with various junctions indicated *[2]*. b) Boundary representation of a scaled down (40%) Y-shaped 3-way junction.

Rather than relying on parametric or equation-based automation, the approach is guided by manual adjustments informed by geometric segmentation strategies.

2.1. Guide Surfaces Based Slicing Framework

Built via visual programming tools in Grasshopper, the core slicing logic is governed by the creation of guide surfaces (the 3D surfaces shown in green, figure 2), which serve as spatial boundaries between which slicing planes or contours are interpolated. These surfaces are manually created in the CAD environment, guided by the shape's curves, any overhanging features, and the direction in which the object will be fabricated (in this case a Y-shaped geometry, shown in turquoise, figure 2). The slicing strategy, planar or non-planar, is selected and adjusted based on the nature and relative shape of these guide surfaces.

- ***Planar slicing*** is employed when the geometry supports uniform or gradually varying build layers. It can be a uniform planar (shown in purple, figure 2) and non-uniform planar.
- ***Non-planar slicing*** is preferred in regions with steep overhangs or junctions, where traditional layering would lead to supporting material build-up or discontinuities. It can be a uniform non-planar and non-uniform non-planar (shown in red, figure 2).

This manual, yet visually intuitive control, allows the designer to localize and customize the slicing behavior with respect to specific design features by tweaking the guide surfaces.

Slicing	Description	Occurrence	Y-Shaped Junction Design
Planar uniform	Layers or slices are flat and evenly spaced throughout	✓	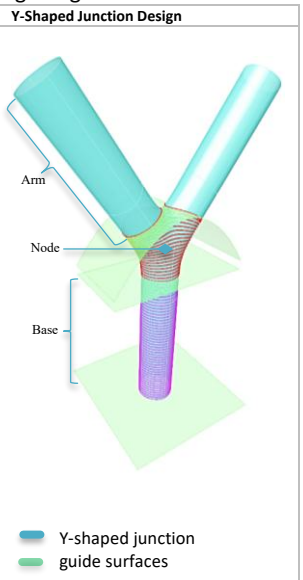
Planar non-uniform	Layers or slices are flat but spacing varies across the geometry.	✗	
Non-planar uniform	Layers or slices follow a curved or varying surface with consistent thickness.	✗	
Non-planar non-uniform	Layers or slices follow a curved or varying surface with variable thickness.	✓	

Figure 2. Guide surfaces for Y-shaped junction in grasshopper algorithm.

2.2. Geometric Decomposition Inspired by Literature

The methodology draws inspiration from *volume decomposition* [3–5] and division based on *neutral axis* of geometries and sub geometries[6–8]**.** Geometries with continuous or near-uniform curvature along a dominant axis are segmented into sub-regions based on observable neutral axes. Each sub-geometry is evaluated for its suitability to planar or non-planar slicing, allowing for selective, localized application of the slicing strategy. This segmentation helps mitigate build failures typically caused by inconsistent path direction or unsupported overhangs, especially at critical nodes such as Y-shaped junctions (e.g., the Bow Window prototype).

2.3. Assumptions and Limitations

- The slicing workflow is not dynamically adaptive; it requires user expertise for guiding surface creation and slicing decisions. However, it has the potential of dynamic adaptability via a similar workflow shared by Jacopo Lettori et al.[9] primarily for uniform and non-uniform planar slicing. It can be adapted and tweaked to accommodate non-planar aspect of slicing as well.
- All slicing logic is implemented in Grasshopper 3D using visual programming, without automatic geometry analysis or feature recognition. To automate the workflow, a future module based on volume decomposition methods [3–5] will enable feature recognition.
- The methodology assumes access to a suitable digital twin or simulated environment for previewing deposition behavior prior to fabrication.
- Tool orientation kinematics are not explicitly modeled; instead, the TacoABB plugin for grasshopper [10] is used, offering inverse kinematics for robot, custom tool orientation, and collision detection.
- The current algorithm does not yet account for process-specific factors such as deposition width or thermal effects. However, this study is part of a broader experimental effort aimed at integrating design-for-WAAM rules.

The presented work is a preliminary study aimed at building foundational expertise and design insight. While it currently has various limitations, namely, its manual nature and the lack of integration of process-specific characteristics, it establishes a basis for future developments. These will include the implementation of (semi-)automated procedures and the integration of design-for-WAAM rules derived from ongoing experimental prototyping activities.

3. Path Planning

To validate and fine tune the accuracy of prepared algorithm within feasible period, one of the most repetitive geometric features, Y shaped junction, was employed for slicing and later, prototyping. This shape offers a viable combination of various slicing types as indicated in figure 2. Additionally, table 1 indicates salient features of representative geometry and its corresponding slicing held common for distinctive path planning approaches discussed in sections 3.1 and 3.2.

Domain	Specification	Magnitude
Geometry	Outer Diameter/mm	18.5
	Height/mm	118
	Arm Span/mm	87
	Overhang Angle /°	45°
Path Planning	Deposition Displacement/mm	2.1
	Layer Height /mm	1
	Slicing (Base of Y-shaped junction)	Planar uniform
	Slicing (Node of Y-shaped junction)	Non-planar non-uniform
	Slicing (Arms of Y-shaped junction)	Non-planar non-uniform

Table 1. Geometry and slicing data of Y-shaped junction.

3.1. Conventional Approach

This mode focused on utilizing most employed methodologies for planar and non-planar path planning.

Weld Start Point

Irrespective of the slicing type, starting points were displaced by one deposition point (2.1 mm). Resultingly, a spiraled pattern of starting points was formed as illustrated in the figure 3a.

Sub-layers

Following the convention, a non-uniform planning approach was maintained specifically for non-planar slicing. Hence, no sub-layers were introduced in this approach. Figure 3b indicates slicing of nodular (where all the neutral axes of the geometry coincide to form a node) region of Y-shaped junction.

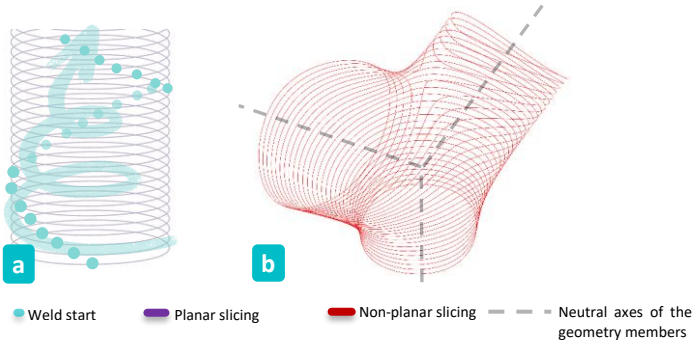

Figure 3. a) Spiralized start point pattern. b) Non-planar slicing of junction without sub-layers.

3.2. Optimized Approach

Validated through series of iterative prototyping attempts, this approach tweaks conventional path planning aimed to obtain better surface finishes and defect free components.

Weld Start Point

For planar slicing, weld start points are rotated by 90° with each layer. This helps mitigate surface waviness caused by excess material deposition at the weld's starting bead, as illustrated in figure 4a. In contrast, for non-planar slicing at nodes, start points are placed at the highest regions of each layer while switching them alternatively between these highest points to maintain component's symmetry. This strategy utilizes the excess material at the start of the weld to fill potential gaps arising from layer non-planarity, particularly near the top of the Y-junction node. These high points are indicated in figure 4b.

Sub-Layers

Regardless of the slicing type, sub-layers are essential for maintaining the geometric conformity of the printed component, especially when intra-layer height varies. In the Y-shaped junction case study, this is particularly relevant for non-planar slicing at the node. Additionally, the use of sub-layers helps fill gaps at the top region of the junction's node, which would otherwise be prone to the formation of macro-voids. These sub-layers are indicated in figure 4b.

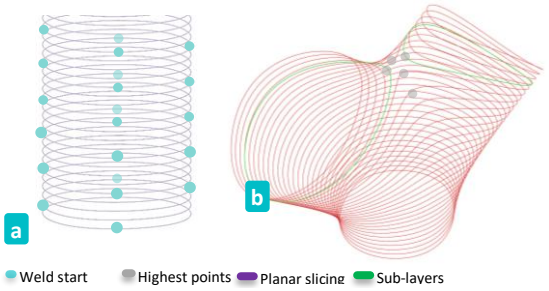

Figure 4. a) Quarterly switching start points. b) Sub-layers and highest points.

4. Prototyping

RocWAAM robotised equipment, located in the Department of Mechanical Engineering at Politecnico di Milano, is a fully integrated WAAM cell for prototyping large-scale metal components. It combines an ABB IRB 2600-12/1.85 robot with a high-precision IRBP 250 positioner provided by ABB. Whereas, the welding hardware is provided by Fronius and Arroweld which includes TPS 400i arc welding system, WF 25i REEL R feeder, SB 60i R buffer, and WF 60i robot torch. The cell is equipped with real-time monitoring sensors and a custom control architecture for precise control of toolpaths, process parameters, and robot motion. Table 2 outlines the technical details of the prototyping process.

Domain	Specification	Magnitude
Material	Welding Wire	AlSi5 (BÖHLER S-Al Si 5)
	Wire Diameter/mm	1.2
	Substrate	Al 6061
	Substrate Size/mm	300 x 300 x 20
Process Parameter	Current/A	91
	Voltage/V	13.6
	Wire Feed Speed (WFS) / m/min	6.5
	Weld Speed (WS) / mm/s	12
	Shielding Gas	Argon (I1 100% Ar)
	Shielding Gas Flow/ L/min	16
	Interlayer Waiting Time / s	90
	Contact Tip to Work Distance (CTWD) / mm	15
	MIG Mode |Cycle |Wait Time/ s	CMT Cycle Step | 5 | 0.05

Table 2. Summary of prototyping data (material specifications and process parameters).

The experimental campaigns for both approaches discussed in 4.1 and 4.2 were conducted using consistent process parameters and materials defined in table 2. Hence, both approaches only vary with respect to path planning.

4.1. Conventional Approach

Although the conventional approach showed promising results, particularly in printing the overhang junction using non-planar slicing, two important observations were noted.

- Spirally oriented start beads leave prominent marks on the surface resulting in poor surface finish (figure 5a, 5b).
- The absence of sub-layers and suboptimal start bead placement caused a macro-void at the junction's centre (figure 5c).

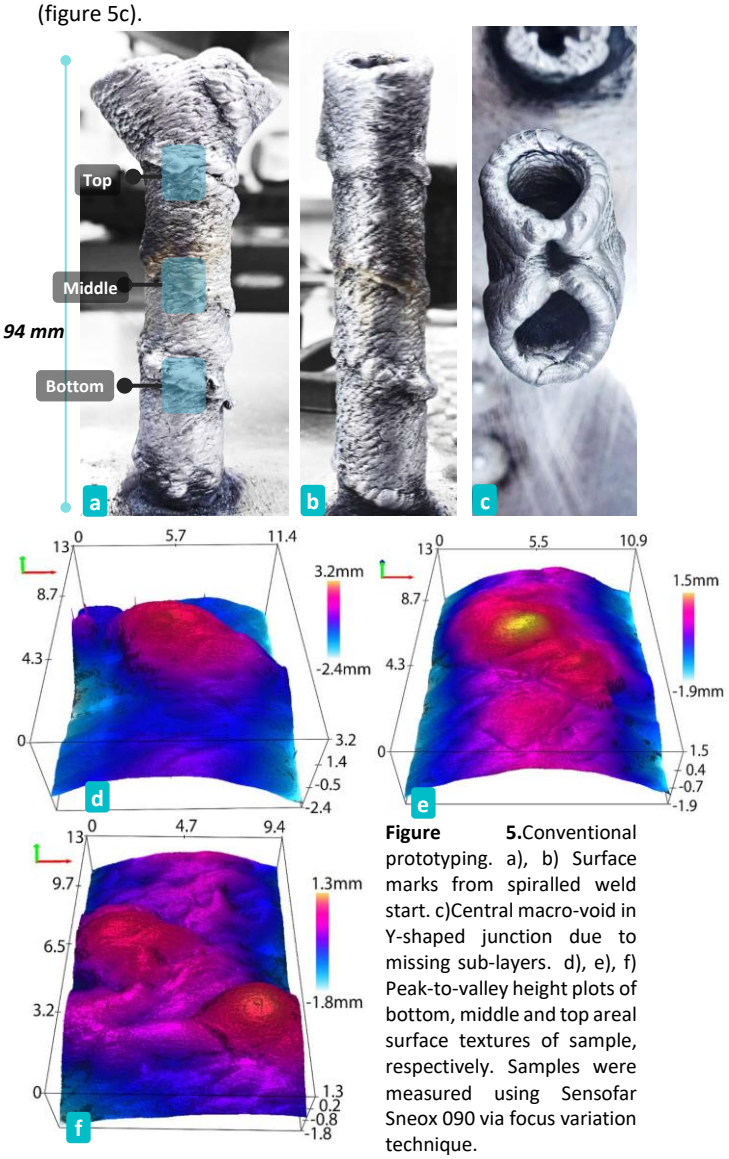

Figure 5. Conventional prototyping. a), b) Surface marks from spiralled weld start. c)Central macro-void in Y-shaped junction due to missing sub-layers. d), e), f) Peak-to-valley height plots of bottom, middle and top areal surface textures of sample, respectively. Samples were measured using Sensofar Sneox 090 via focus variation technique.

4.2. Optimized Approach

Presence of macro-voids can lead to stress concentrations under loading conditions, potentially resulting in structural failure of the structural component. The observations from section 4.1, however, were addressed via optimized approach elaborated in section 3.2. Resulting geometry showed following salient features:

Planar Base: The spirally oriented start bead overdeposition was eliminated by quarterly alternating the start point per layer, improving surface finish. However, the texture remained rough with a scaly feel (figure 6a).

Junction: Prototyping was conducted in two stages. Alternating start points at the highest spots without sub-layers improved void filling but left minor gaps (figure 6b). Adding two sub-layers (figure 4b) eliminated central voids, though material buildup appeared in overhang areas, likely from overlap between sub-layers and main layers (figure 6c).

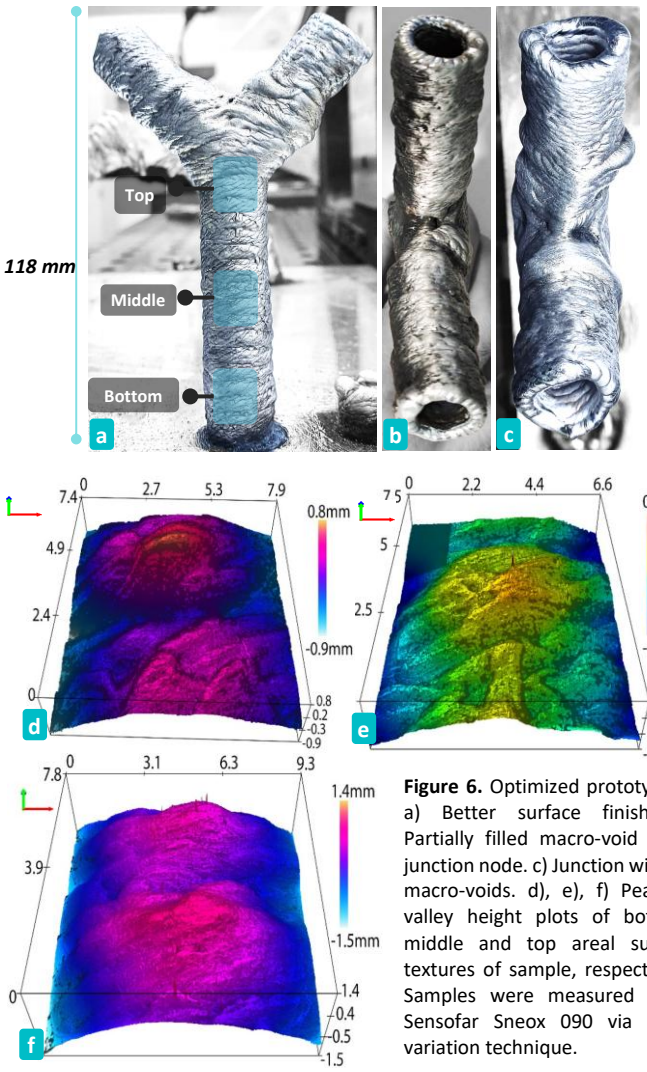

Figure 6. Optimized prototyping. a) Better surface finish. b) Partially filled macro-void in Y-junction node. c) Junction with no macro-voids. d), e), f) Peak-to-valley height plots of bottom, middle and top areal surface textures of sample, respectively. Samples were measured using Sensofar Sneox 090 via focus variation technique.

5. Discussion

Monochromatic top-view images of each sample were captured using a Mitutoyo Quick Vision Pro QV202-PT5F to evaluate diametral accuracy. Each data set comprised ten external diameter measurements taken at constant intervals along the base of each sample using SolidWorks 2D Sketch. Mean diametral errors were 0.4 mm for the optimized approach and 0.7 mm for the conventional one. Furthermore, the geometry printed with optimized approach was scanned using a GoScan 3D handheld scanner (0.8 mm resolution). As shown in figure 8, the results reveal:

- A ~5.0 mm deviation occurred in the junction's overhang, likely from excess material between closely spaced layers, affecting its thermal distribution.[11]
- A ~2.5 mm offset in one arm extension, likely due to a minor mismatch between the actual and defined rotation centers in the Grasshopper algorithm.

Surface roughness was assessed using a Sensofar S Neox 090 via the focus variation technique. The measured areal roughness (Sa) values for the regions shown in figures 5d–f and 6d–f are presented in figure 7. The results indicate that the optimized approach mostly produced a smoother surface finish than the conventional one.

6.Conclusion and Future Development

This work presents a flexible and customizable WAAM workflow that simplifies the prototyping of complex and organic metal geometries.

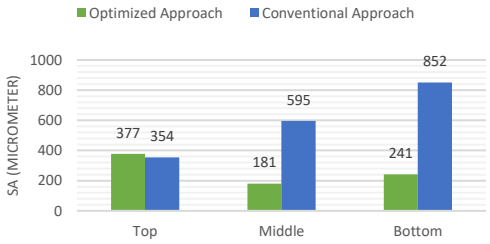

Figure 7: Areal average roughness (Sa) for optimized and conventional approach samples along their bottom, middle, and top regions. (See figure 5-6)

It enables industrial designers to validate concepts earlier with respect to design for manufacturability (DFM), bridging the gap between digital design and physical fabrication. The approach expands creative freedom while maintaining process control through visual and parametric slicing and toolpath generation. Future developments will include:

- Adaptive non-planar slicing inspired by planar methods.
- Including thermal effects and deposition width in slicing logic.
- Enhanced simulation environments for toolpath validation.
- Experimental tuning to define design-for-WAAM rules.

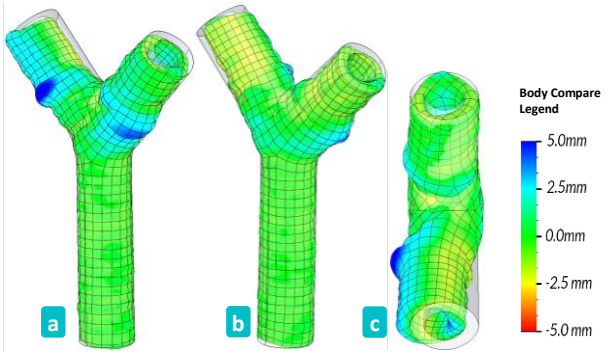

Figure 8. Optimized Prototyping vs. ideal geometry a) Isometric view I, b) Isometric view II, c) Top view.

Acknowledgments

This work is part of the RocWAAM project at Politecnico di Milano's department of Mechanical Engineering. The authors thank Edilanzutti S.p.A. for commissioning this study, ABB, Fronius, and Arroweld for hardware and support, and Voestalpine Böhler Welding GmbH for weld wire supply. Thanks are also extended to the RocWAAM team, and to BLM group for 3D scanning support.

References

[1] Müller, J, Hensel, J, 2023. WAAM of structural components—building strategies for varying wall thicknesses. *Weld World* 67, 833–844. https://doi.org/10.1007/s40194-023-01481-y

[2] Causi, L, n.d. Design & prototyping for waam: a light deflective bow window.

[3] Zhao, G, Ma, G, Feng, J, Xiao, W, 2018. Non-planar slicing and path generation methods for robotic additive manufacturing. Int J Adv Manuf Technol 96, 3149–3159. https://doi.org/10.1007/s00170-018-1772-9

[4] Yuan L, Ding, D, Pan, Z, Yu, Z, Wu, B, Van Duin, S, Li, H, Li, W, 2020. Application of multidirectional robotic wire arc additive manufacturing process for the fabrication of complex metallic parts. IEEE Trans. Ind. Inf. 16, 454–464. https://doi.org/10.1109/tii.2019.2935233

[5] Ding, D, Pan, Z, Cuiuri, D, Li, H, Larkin, N, Van Duin, S, 2016. Automatic multi-direction slicing algorithms for wire based additive manufacturing. Robotics and Computer-Integrated Manufacturing 37, 139–150. https://doi.org/10.1016/j.rcim.2015.09.002

[6] Gu, X, Hou, Z, Xu, J, Chen, K, Zhang, G, n.d. A novel additive manufacturing method for spiral parts.

[7] Nguyen, L, Buhl, J, Bambach, M, 2018. DECOMPOSITION algorithm for tool path planning for wire-arc additive manufacturing. Journal of Machine Engineering Vol.18, 96–107. https://doi.org/10.5604/01.3001.0010.8827

[8] Ruan, J, Sparks, TE, Panackal, A, Liou, FW, Eiamsa-ard, K, Slattery, K, Chou, H-N, Kinsella, M, 2007. Automated slicing for a multiaxis metal deposition system. Journal of Manufacturing Science and Engineering 129, 303–310. https://doi.org/10.1115/1.2673492

[9] Lettori, J, Raffaeli, R, Borsato, M, Pellicciari, M, Peruzzini, M, 2023. Non-uniform planar slicing for robot-based additive manufacturing. CADandA 104–118. https://doi.org/10.14733/cadaps.2024.104-118

[10] Taco abb [WWW Document], 2016. Food4Rhino. URL https://www.food4rhino.com/en/app/taco-abb (accessed 7.10.25).

[11] Müller, Johanna, Constantinos Goulas, and Jonas Hensel, 2024. Analysis of Thermal Cycles during DED-Arc of High-Strength Low-Alloy Steel and Microstructural Evolution.. Journal of Materials Research and Technology: 3661–74. https://doi.org/10.1016/j.jmrt.2024.07.066.